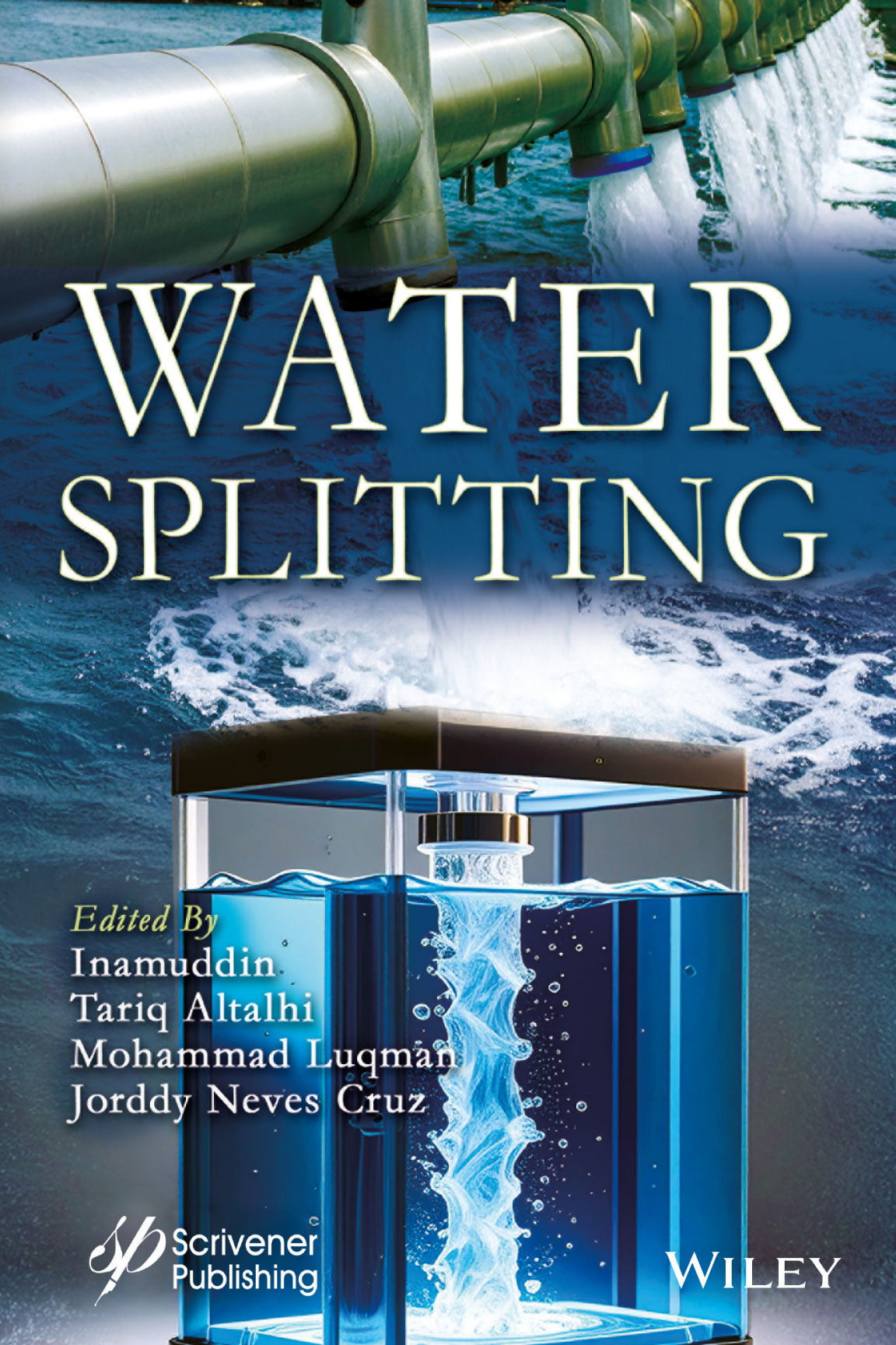
WATER
SPLITTING
Edited By
Inamuddin
Tariq Altalhi
Mohammad Luqman
Jorddy Neves Cruz
Scrivener Publishing
WILEY

Water Splitting

Scrivener Publishing
100 Cummings Center, Suite 541J
Beverly, MA 01915-6106

Publishers at Scrivener
Martin Scrivener (martin@scrivenerpublishing.com)
Phillip Carmical (pcarmical@scrivenerpublishing.com)

Water Splitting

Production of Hydrogen

Edited by

Inamuddin

Tariq Altalhi

Mohammad Luqman

and

Jorddy Neves Cruz

WILEY

This edition first published 2025 by John Wiley & Sons, Inc., 111 River Street, Hoboken, NJ 07030, USA and Scrivener Publishing LLC, 100 Cummings Center, Suite 541J, Beverly, MA 01915, USA

For more information about Scrivener publications please visit www.scrivenerpublishing.com.

Wiley Global Headquarters
111 River Street, Hoboken, NJ 07030, USA

For details of our global editorial offices, customer services, and more information about Wiley products visit us at www.wiley.com.

The manufacturer's authorized representative according to the EU General Product Safety Regulation is Wiley-VCH GmbH, Boschstr. 12, 69469 Weinheim, Germany, e-mail: Product_Safety@wiley.com

Library of Congress Cataloging-in-Publication Data

ISBN 9781394247622

Cover image: Generated with AI using Adobe Firefly
Cover design by Russell Richardson

Set in size of 11pt and Minion Pro by Manila Typesetting Company, Makati, Philippines

Printed in the USA

10 9 8 7 6 5 4 3 2 1

Contents

Preface

Water splitting for the production of hydrogen is a rapidly evolving field at the forefront of interdisciplinary research and industrial development. It encompasses the integration of multiple scientific disciplines, including chemistry, physics, materials science, engineering, and environmental science, to address the global energy challenge and transition towards a sustainable future. In the context of disciplinary development, water splitting has witnessed significant advancements in understanding the fundamental principles and kinetics of the process. Researchers have explored various methods and catalysts for efficient water splitting, aiming to enhance hydrogen production rates and minimize energy consumption. The field of electrocatalysis has seen remarkable progress, with the development of novel materials, such as metal oxides, metal sulfides, and molecular catalysts, to enhance the performance of electrolyzers. Furthermore, the emergence of photoelectrochemical water splitting has brought together materials science, electrochemistry, and photonics. Researchers have been exploring semiconductor materials, such as metal oxides and metal chalcogenides, to design efficient photoelectrodes capable of harnessing solar energy for water splitting. The field has witnessed breakthroughs in bandgap engineering, surface modification, and tandem cell configurations, enabling improved solar-to-hydrogen conversion efficiency. In terms of industry development, water splitting holds immense potential for sustainable hydrogen production, which can be used as a clean energy carrier. The advancement of water electrolysis technologies, such as alkaline and proton exchange membrane (PEM) electrolyzers, has enabled scalable and cost-effective hydrogen production. These technologies are being increasingly deployed in industries, such as hydrogen fueling stations, energy storage systems, and industrial processes, to meet the growing demand for clean energy solutions. Moreover, the integration of water splitting with other renewable energy sources, such as solar and wind, presents opportunities for the development of integrated systems and the establishment of a hydrogen economy. The ability to store and utilize hydrogen as a versatile

energy carrier has the potential to revolutionize sectors like transportation, power generation, and industrial applications, enabling a transition away from fossil fuels and reducing carbon emissions.

Water Splitting: Production of Hydrogen book provides a comprehensive exploration of water splitting, starting with foundational principles on thermodynamics and kinetics, crucial for understanding hydrogen production. It covers diverse methods and catalysts, emphasizing material selection and reaction optimization. Advancing further, the text explores recent innovations in materials and catalysts tailored for water splitting, highlighting synthesis techniques, functional materials, and nanotechnology integration. Detailed insights into electrochemical water splitting, encompassing alkaline and proton exchange membrane (PEM) electrolysis, clarify design principles, operational strategies, and electrolyte enhancements. A significant portion is dedicated to water photoelectrochemistry, analyzing semiconductor materials, photoelectrode design, and solar-to-hydrogen conversion strategies. The book delves into integrated systems, advanced reactors, and the role of artificial intelligence, machine learning, and big data in enhancing water splitting technologies. Concluding with applications, it explores hydrogen's potential as a clean energy carrier in fuel cells, energy storage, and industrial processes. Addressing gaps in current resources, the book focuses on cutting-edge advancements, ensuring researchers stay informed and prepared to contribute to the field's progress. The chapters included in the book are summarized below:

Chapter 1 explores the fundamental thermodynamical principles governing the energy requirements and efficiencies of splitting water molecules into H2 and O2. The thermodynamical parameters discussed include Gibbs free energy, enthalpy, and entropy changes, emphasizing their implications for developing efficient, effective, and sustainable hydrogen production techniques.

Chapter 2 emphasizes the importance of understanding water splitting kinetics for developing efficient catalysts for green energy. It explores the distinct mechanisms of the Oxygen Evolution Reaction (OER) and the Hydrogen Evolution Reaction (HER), discusses various tools for studying their kinetics, and highlights the need for systematic investigation to optimize catalyst design in both alkaline and acidic media.

Chapter 3 presents a comprehensive study of perovskite electrocatalysts for water splitting. Hydrogen fuel from electrochemical water splitting using renewable electricity is a promising future energy source. Effective, stable electrocatalysts are essential for improving water splitting reaction rates. This chapter reviews recent advances in perovskite oxides for catalytic

reactions, exploring their mechanisms, composition, and design strategies, including insights from density functional theory.

Chapter 4 explores electrode materials, especially those based on titania nanotubes, that can be used in solar-driven electrochemical water splitting. As water splitting is considered a promising field for the green production of hydrogen, the accurate selection and design of photoelectrodes are of key importance.

Chapter 5 discusses the recent advances of MXenes materials in the electrocatalytic production of hydrogen and oxygen. Strategies include the control of surface terminating groups and structural as well as heteroatom doping, targeting improvements in the catalytic performance of MXenes towards efficient water splitting.

Chapter 6 discusses inorganic photocatalysts for hydrogen production through water splitting, emphasizing the importance of their crystalline structure and semiconductors like TiO2. It covers the fundamental principles of photocatalysis and the physical and chemical properties of photocatalysts. The chapter also explores methods to improve water splitting efficiency, addressing current challenges and prospects.

Chapter 7 surveys contemporary water splitting materials and discusses future requirements in the field. Considering the functional materials used for water separation, the most efficient functional material is determined with the help of the analytical hierarchy process. This chapter is designed to assist industry professionals and specialists in selecting the optimal group of materials for hydrogen production through water splitting.

Chapter 8 focuses on utilizing nanotechnology to advance the field of water splitting. This research area explores how nanoscale materials and structures can be engineered to enhance the efficiency and effectiveness of splitting water molecules into hydrogen and oxygen gases, a process crucial for renewable energy production and sustainable fuel generation. Key objectives include improving catalyst performance, optimizing light absorption for photoelectrochemical cells, and exploring new nanomaterials for electrolysis. Overall, nanotechnology in water splitting research aims to contribute to cleaner energy technologies and address global energy challenges.

Chapter 9 explores hydrogen utilization through fuel cells, emphasizing thermodynamics, kinetics, and various types of fuel cells (acidic, alkaline, phosphoric acid, and high-temperature). It covers electrocatalysts, proton exchange membranes, and porous electrodes. Challenges like hydrogen transport are discussed, highlighting the importance of fuel cells in achieving a carbon-free society.

Chapter 10 discusses catalysts for the anodic oxygen evolution reaction. It covers the advantages, disadvantages, and future perspectives of the catalyst types discussed in the literature. Additionally, the characterization of the catalyst in anodic oxygen evolution is included.
Chapter 11 delves into the characterization and analysis of electrolyzer performance, emphasizing mechanisms that enhance efficiency and inform material selection. This comprehensive study covers key aspects including current density, Faraday efficiency, energy efficiency, stability, as well as gas production rates and purity, providing crucial insights for improving system performance.

1

Thermodynamics of Electrochemical Water Splitting

Manash P. Nath[1,2], Manju Kumari Jaiswal[1,2], Suvankar Deka[1,2] and Biswajit Choudhury[1,2]*

[1]Materials and Energy Laboratory, Physical Sciences Division, Institute of Advanced Study in Science and Technology (IASST), Assam, India
[2]Academy of Scientific and Innovative Research (AcSIR), Ghaziabad, India

Abstract

The thermodynamics of water splitting elucidates the intricate balance of energy transformations fundamental to this crucial reaction, including photocatalytic and electrocatalytic water splitting. Electrocatalytic water splitting—triggered by the application of an external voltage—holds great potential for creating sustainable energy-producing hydrogen gas (cathode) and oxygen (anode). It requires overcoming the thermodynamic barriers, such as enthalpy change (ΔH) and Gibbs free energy change (ΔG), associated with the bond dissociation energies of water molecules and the formation of intermediates. Gibbs free energy barrier (ΔG) must be negative to proceed with the water splitting reaction spontaneously. At this hour, electrocatalysts play a pivotal role in decreasing the activation energy barrier enhancing the water splitting kinetics, and increasing the overall efficiency. Noble metal-based electrocatalysts such as platinum (Pt), ruthenium (Ru), and iridium (Ir) have been employed for their high catalytic activity with an extremely low free energy barrier. However, their expensiveness and scarcity have instigated researchers to search for low-cost earth-abundant electrocatalysts such as transition metal oxides, sulfides, phosphides, and high entropy alloys, among others. Therefore, the study provides an in-depth and comprehensive understanding of various thermodynamic parameters associated with the electrocatalytic water splitting process.

***Keywords*:** Electrochemical, gibbs free energy, noble metal, layered materials

**Corresponding author*: biswajitchoudhury@iasst.gov.in; biswa.tezu@gmail.com

Inamuddin, Tariq Altalhi, Mohammad Luqman and Jorddy Neves Cruz (eds.) Water Splitting: Production of Hydrogen, (1–22)

1.1 Introduction

The worldwide energy crisis and the related ecological problems have spurred scientists to seek the replacement of fossil fuels with renewable energy sources [1, 2]. Natural resources, such as energy generated by the sun or wind and water splitting technologies, offer an enticing means of producing hydrogen sustainably [3]. Water splitting involves the breaking down of water molecules into H_2 and O_2 under the effect of an external energy source such as a high temperature, light, or the application of an electric field [4]. From an environmental perspective, three approaches are mostly adopted for water splitting. These approaches are (a) photocatalytic, (b) electrocatalytic, and (c) photoelectrocatalytic. Photocatalytic water splitting requires a semiconductor with a high absorption cross section for incident solar photons to excite photocarriers and generate free electrons and holes [5]. For overall splitting, a semiconductor's conduction and valence band edge potential must be suitable enough to carry out the oxidation/reduction of water. In the ideal case, the band gap must exceed the minimum water splitting potential of 1.23 V [6]. Electrocatalytic water splitting involves H_2 generation (hydrogen evolution reaction or HER) and O_2 generation (oxygen evolution reaction or OER). The first electrolytic cell was proposed in 1789, and it comprises three parts: cathode, anode, and electrolyte [7]. Two moles of hydrogen and oxygen are produced from the splitting of 1 mol of water. It is an endothermic, non-spontaneous process with a standard Gibbs free energy change ($\Delta G = +237.3$ kJ/mol) [8]. Photoelectrocatalytic water splitting (PEC) is an electrocatalytic water splitting process with additional energy provided by light [9]. For photoelectrode materials to be commercially viable, they must have an STH, i.e., solar-to-hydrogen conversion efficiency of above 10% in addition to being sufficiently abundant on Earth and stable in water [10]. In 1972, Honda and Fujisima demonstrated the first PEC with TiO_2 photoanode [11].

The efficacy and feasibility of catalytic water splitting are enthalpy, entropy, and Gibbs free energy. Since the water splitting process is endothermic or uphill, its high ΔG of +237 kJ/mol is overcome by providing electrical energy equivalent to 1.23 V and increasing the temperature to accelerate the reaction [12]. To achieve it, the entire enthalpy requirement of $\Delta H = -283.85$ kJ/mol comes from the environment at temperature T as temperature T is necessary to achieve the required work $T\Delta S$, which is important for the electrolysis of water [13]. The first law of thermodynamics, "the law of energy conservation," describes how external energy (light, electricity, or heat) must be added to disintegrate the chemical bonds that bind water molecules, thereby converting

them into H_2 and O_2 [14]. On the other hand, the second law of thermodynamics describes that the water splitting process is not 100% efficient with a positive entropy. A temperature equivalent to (T) >4,500 K can be used to split water, which is a maladroit process. Gibbs free energy change (ΔG), which describes the spontaneity of a water splitting reaction, becomes negative at T >4,500 K or E (V) >1.23 V, which indicates a favorable water splitting process [15]. Several attempts have been made to eliminate the internal energy losses that arise from overpotential and cell resistances to minimize the energy requirements of an electrolytic cell [16]. They include controlling the electrolyte's temperature, pressure, and chemical potential [16]. Thus, all three thermodynamic parameters, H, S, and G, are dependent on temperature (T) and pressure (P) and will describe the feasibility of an electrochemical water splitting system. In the case of HER, i.e., hydrogen evolution reaction, the change in the thermodynamic parameters (ΔH, ΔS, and ΔG) depends on the electrolytic conditions, i.e., acidic or alkaline. The abundance of protons (H^+), in the case of acidic electrolytes, makes the Volmer step rate determining [17]. In alkaline conditions, H_2O adsorption and dissociation occur before the Volmer step (adsorption of H). This is similar to OER, where the chemical environment (i.e., acidic or alkaline) determines the oxidation of water [18].

1.2 Thermodynamic Parameters

1.2.1 Enthalpy (H)

It is the system's overall heat content. Thus, the change in the enthalpy (ΔH) of a system consists of two parts, which are the requirements of thermal energy (ΔQ) and useful work done (ΔW). The overall equation can be written as follows:

$$\Delta H = \Delta Q \pm \Delta W \tag{1.1}$$

A positive change in enthalpy describes an endothermic reaction, whereas a negative change describes an exothermic reaction.

1.2.2 Entropy (S)

The entropy, a state function, measures the reaction system's overall degree of disorder or unpredictability. The relationship provides the shift in entropy (S).

$$\Delta S = \Delta Q/T \tag{1.2}$$

A more considerable change in entropy with input energy indicates that the system is away from the thermodynamic equilibrium, i.e., it is highly disordered, i.e., chaotic or spontaneous. It is directly dependent upon temperature. In the case of water splitting, H_2O (liquid) is broken down into gas H_2 and O_2, which increase the entropy of the system.

1.2.3 Gibbs Free Energy

Gibbs free energy describes the thermodynamic potential to determine the maximum work performed by a closed system in isothermal and isobaric conditions. Gibbs free energy change (ΔG) is the maximum amount of work that can be obtained from a closed system that can exchange heat and interact with its surroundings, i.e.,

$$\Delta G = -\Delta W \tag{1.3}$$

Therefore, upon switching Equations 1.2 and 1.3 in Equation 1.1, we obtain the following:

$$\Delta G = \Delta H - T\Delta S \tag{1.4}$$

The ΔG^o of water splitting is obtained under the standard temperature "T" = 398 K, pressure "P" = 1 bar, and concentration = 1 M. If ΔG is negative under these standard conditions, the water splitting process is both spontaneous and thermodynamically favorable. The equilibrium constant "K" of the system is relatable to the Gibbs free energy change (ΔG) by the following:

$$\Delta G = -RT\ln K \tag{1.5}$$

If ΔG decreases, the equilibrium constant "K" of the chemical reaction increases. If $\Delta G < 0$, the spontaneity of the chemical reaction increases.

1.3 Thermodynamics of Water Splitting

Water dissociation, which comprises liquid water and water vapor, decomposes into its elemental compositions (H_2 and O_2) according to the following:

Table 1.1 The thermodynamic parameters of liquid and gaseous H_2O.

Parameters	Liquid (H_2O)	Vapor (H_2O)
ΔH_{H2O}^{o} kJ mol^{-1}	+285.840	+241.80
ΔS_{H2O}^{o} J mol^{-1} K^{-1}	+163.15	+44.10
ΔG_{H2O}^{o} kJ mol^{-1}	+237.22	+228.66

$$H_2O \rightarrow H_2 + 1/2O_2 \tag{1.6}$$

Under the standard conditions of temperature (T^o = 298 K) and pressure (P^o = 1 bar) for water, the thermodynamic parameters of enthalpy (ΔH_{H2O}^{o}), entropy (ΔS_{H2O}^{o}), and Gibbs free energy (ΔG_{H2O}^{o}) change are given in Table 1.1 [15].

The dissociation of water is highly endothermic and non-spontaneous, although the entropy conditions are favorable for water splitting. When there is a conversion in the state of matter from water (liquid) to gas (steam), the entropy increases from +44.1 to +228.66 J mol^{-1} K^{-1}, which decreases enthalpy and Gibbs free energy. All the three parameters ΔH^o, ΔS^o, and ΔG^o for water splitting depend on the temperature (T) and pressure (P) of the system through the following relation 1.7 [12]:

$$\Delta G\,(T, P) = \Delta H\,(T, P) - T\Delta S\,(T, P) \tag{1.7}$$

when water produces H_2 and O_2 due to water electrolysis, the electrical energy of $-\Delta G$ and a heat transfer of $-T\Delta S$ are required. The enthalpy voltage (V) and the water electrolysis voltage (E) connected with the enthalpy (ΔH) and free energy change (ΔG) are given by the following:

$$-\Delta H = nFV$$

$$-\Delta G = nFE \tag{1.8}$$

where "F" equals the Faraday constant of 96,485 C/mol, and n = 2 is the number of transferred electrons. Under ideal cases at STP conditions, "V" equals 1.23 V, and "E" equals 1.48 V [12]. But in non-ideal cases when an overpotential (η) is used, external heat is not required because of the

participation of electrical energy in both $-\Delta G$ and $-T\Delta S$. Here, the voltage is called thermo-neutral voltage [12]. Thus, the enthalpy change (ΔH) can be expressed in terms of the enthalpies of the three phases involved as follows [16]:

$$\Delta H = H \text{ (wet hydrogen)} + H \text{ (wet oxygen)} - H \text{ (reagent water)} \tag{1.9}$$

Here, the hydrogen and oxygen are assumed to be wet because water vapor is mixed with them. For the continuous production of H_2 and O_2, there is a continuous requirement for reagent water in the amount of $1 + 1.5P_w/(P - P_w)$, where the products of the process consist of 1 mol of hydrogen mixed with $P_w/(P - P_w)$ mol of water vapor at an overall pressure P, and 0.5 mol of oxygen mixed with $0.5P_w/(P - P_w)$ mol of water vapor, also at an overall pressure P [16].

1.4 Factor Dependence on the Thermodynamics of Water Splitting

1.4.1 Temperature

The thermodynamic parameters, consisting of H, S, and G, are all functions of the operating temperature (T). As seen in Figure 1.1, upon increasing the temperature in the system, the Gibbs free energy change (ΔG) decreases, although the enthalpy (ΔH) remains constant [15].

A decreasing value of ΔG indicates that water dissociation will consume less electrolysis voltage. The enthalpy and Gibbs free energy change in the water dissociation process, as given in relation 1.10 concerning temperature, are determined by the equations given below:

$$\Delta H\,(T) = H_{H2}\,(T) + 1/2H_{O2}\,(T) - H_{H2O}\,(T)$$

$$\Delta G\,(T) = G_{H2}\,(T) + 1/2G_{O2}\,(T) - G_{H2O}\,(T)$$

$$\Delta S\,(T) = S_{H2}\,(T) + 1/2S_{O2}\,(T) - S_{H2O}\,(T) \tag{1.10}$$

The ΔG, which is a function of the temperature ($\Delta G\,(T)$), can be directly used to determine the thermodynamic voltage of water splitting ($E\,(T)$) using the relation $E\,(T) = \Delta G\,(T)/nF$, where $F = 96{,}500$ C mol^{-1}. When T

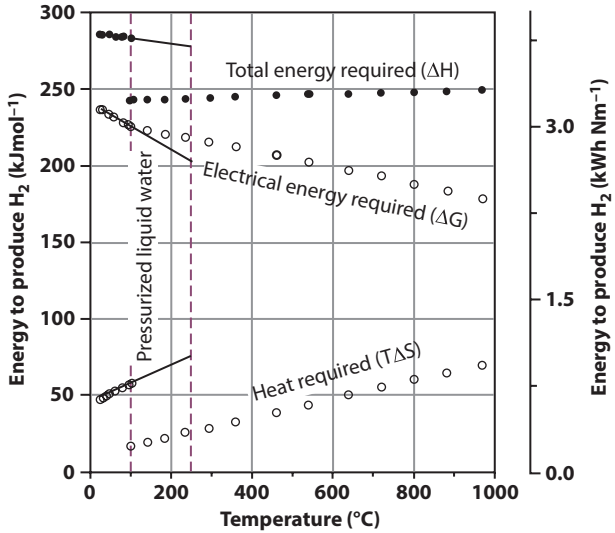

Figure 1.1 Production of H_2 under constant pressure of 1 bar and temperature ranging from 0°C to 1,000°C. *Reproduced with permission from Ref. [15]. Copyright (2015) Willey.*

> 3,000 K, the free energy electrolysis voltage E(T) drops from 1.23 V at 25°C to 1.18 V at 100°C and −0.9 V at 1,000°C. Electricity is not required to dissociate the water molecules [15].

1.4.2 Pressure

The thermodynamic parameters are quite dependent on the pressure of the electrolyzer. For commercial use, the electrolyzers are operated at pressures between 1 and 50 bars, or water splitting occurs at atmospheric pressures, and the output hydrogen gas is kept in compressed vessels for further use. Under isothermal conditions, the relationship between the thermodynamic voltage of water splitting (E) and the pressure over the electrolyzer is given by the following [15]:

$$(\delta E/\delta P)_T = 1/nF\ (\delta \Delta G/\delta P)_T \tag{1.11}$$

The variation of E with pressure (P) at a particular temperature T°C is shown in Figure 1.2 [14]. The effect of the pressure above the electrolyzer on the water splitting (E) thermodynamic voltage is significant (+200 mV at 25°C when the pressure is increased from 1 to 700 bar).

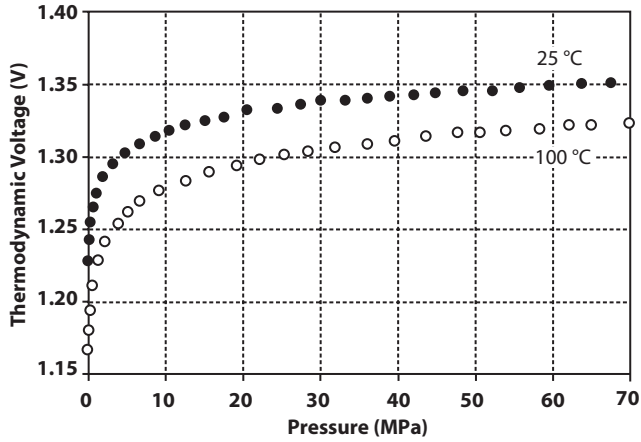

Figure 1.2 Variation of thermodynamic voltage of water splitting with pressure under three different isothermal conditions. *Reproduced with permission from Ref. [15]. Copyright (2015) Willey.*

1.5 Applications in Electrolysis

1.5.1 Hydrogen Evolution Reaction (HER)

The HER process occurs either through Volmer–Heyrovsky or Volmer–Tafel reaction on a HER active site. The Volmer or electrosorption step determines the adsorption of a nascent H in the HER active site (M) forming an adsorbed hydrogen (H_{ads}). It is followed by the release of the H_2 molecule either through Heyrovsky (electrochemical) or Tafel (chemical) desorption mechanisms [19]. The HER mechanism occurring in acidic and alkaline mediums is described below:

i) Electrochemical adsorption of hydrogen (Volmer reaction)

$$H^+ + M + e^- \rightarrow M\text{–}H_{ads}\ (\text{acidic})$$
$$\text{Or}$$
$$H_2O + M + e^- \rightarrow M\text{–}H_{ads} + OH^-\ (\text{alkaline})$$

ii) Electrochemical desorption of hydrogen (Heyrovsky reaction)

$$M\text{–}H_{ads} + H^+ + e^- \rightarrow M + H_2\ (\text{acidic})$$
$$\text{Or}$$

$$M–H_{ads} + H^+ + e^- \rightarrow M + H_2 + OH^- \text{ (alkaline)}$$

iii) Chemical desorption of hydrogen (Tafel)

$$2M–H_{ads} \rightarrow M + H_2$$

In the first step, the change in enthalpy (ΔH) before and after H adsorption over an electrochemical active site is obtained, which is followed by the release of the H_2 molecule.

$$\Delta H_{H,\,ads} = H_{H,\,ads} - H_{site} - 1/2H_{H2} \tag{1.12}$$

where $\Delta H_{H,\,ads}$ is the change in the enthalpy of H adsorption over a site, $H_{H,\,ads}$ is the enthalpy of the site after H adsorption, H_{site} is the enthalpy of the active site before H adsorption, and H_{H2} is the enthalpy of the H_2 molecule. A more negative $\Delta H_{H,\,ads}$ indicates stronger binding strength between an intermediate and a catalyst's active site with better thermodynamic stability. The HER barrier depends on the intermediate state energy of an H adsorbed on the catalyst followed by the release of an H_2 molecule given by ref. [20]. Therefore, the HER performance can be assessed through ΔG_H, i.e., the Gibbs free energy change of the adsorbed hydrogen. The Gibbs free energy change of H adsorption is given by the following:

$$\Delta G_H = \Delta H_{H,\,ads} + \Delta H_{ZPE,\,ads} + T\Delta S_H \tag{1.13}$$

Here, $\Delta H_{H,\,ads}$ is the enthalpy change after H adsorption, $\Delta H_{ZPE,\,ads}$ is the zero point energy change after H adsorption, and ΔS_H is the entropy change of H adsorption given by $\Delta S_H = -0.5S_{H2}$, which is equivalent to 130 J mol^{-1} K^{-1}. "T" is the temperature under standard conditions, i.e., 298 K. ΔG_H is a crucial parameter to describe the HER activity of a catalyst in an acidic medium despite the existence of obstacles (Figure 1.3a) [21]. As shown in Figure 1.3b, alkaline HER requires the H_2O molecule to be adsorbed at the active site, dissociate into H and OH, adsorb H (Volmer step), and release H_2 [22]. It introduces an extra energy barrier (ΔG_B) that controls the overall reaction rate. Thus, its rate becomes considerably slower in alkaline than in acidic conditions. Hence, ΔG_H cannot directly determine a catalyst's HER activity in an alkaline medium. The Bronsted–Evans–Polanyi (BEP) relationship describes that the activation energy of a chemical reaction is directly proportional to its enthalpy change (ΔH). A low activation barrier indicates strong adsorption [23]. Therefore, in the case of alkaline HER, three factors are considered as follows: a) neither too

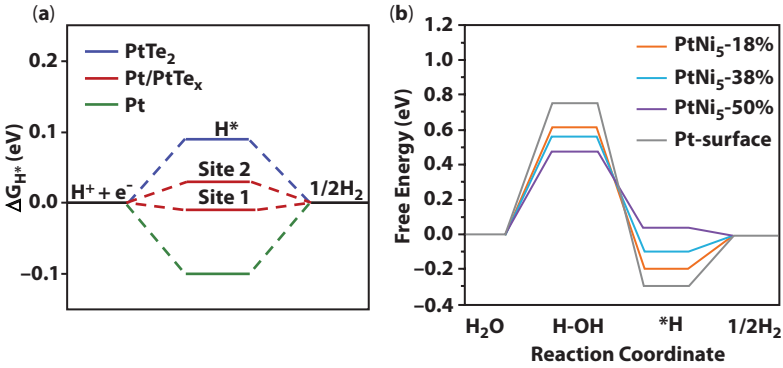

Figure 1.3 Gibbs free energy diagram of (a) acidic HER. *Reproduced with permission from Ref. [21]. Copyright (2021) Elsevier.* (b) alkaline HER. *Reproduced with permission from Ref. [22]. Copyright (2021) Wiley.*

high nor low H binding, b) low water dissociation barrier, and c) low OH binding energies. The ΔG_H for different materials is based on the Norskov reaction of H_2 formation, i.e., $H^+ + * \rightarrow 1/2H_2$. The resultant is a "Volcano" plot given in Figure 1.4 [24, 25]. It follows the Sabatier principle, which describes that for strong HER kinetics, the binding strength between the intermediates and the active site in the catalyst must "neither be too strong nor too weak." For the elements situated in the left, H adsorption becomes "strong" as ΔG_H values tend to be more negative, while for the elements located in the right, the adsorption becomes "weak" as ΔG_H values tend to be more positive. The ideal HER materials are those that are being placed at the peak of the volcano plot [25].

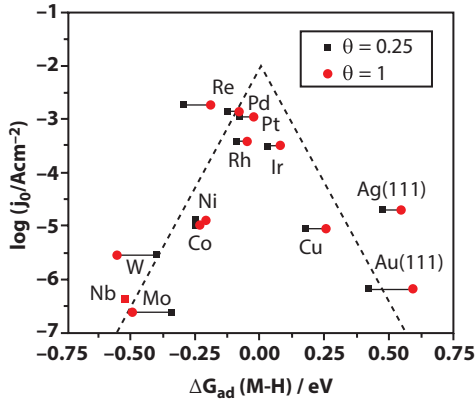

Figure 1.4 Volcano plots of materials in accordance with M–H bond strength. *Reproduced with permission from Ref. [25]. Copyright (2016) Wiley.*

The noble metal Pt is considered the most widely active catalyst toward acidic HER with ΔG_H nearly equal to zero as mentioned above. However, these noble metals are costly and rarely available, so many researchers are eager to investigate and develop a stable, effective electrocatalyst with lower noble metal concentrations for HER. In this regard, noble metals have been investigated for HER, including rhodium (Rh), ruthenium (Ru), and iridium (Ir) [26–34]. Chen *et al.* adopted a gas-controlled method using H_2/O_2/Ar gases to synthesize free-standing Ru nanoparticles, nanowires, and nanosheets, respectively. He studied theoretically the adsorption of hydrogen atoms on Ru crystal facets viz. Ru (001), Ru (100), and Ru (101) by varying the hydrogen coverage over the Ru surface. He found that introduction of H_2 into the crystal planes of Ru makes the system more active as it accelerates the reduction rate of Ru and thus enhances the HER process. According to DFT calculations, the ΔG_H value obtained for Ru on its various crystal planes is in the following order: (101) > (100) > (001). This suggests that the surface effect of the crystals is mostly responsible for the HER performance of Ru NCs [26]. Zhang *et al.*, synthesized ultrafine Ru nanocrystals uniformly distributed on mesoporous Mo_2N nanorods (Ru–Mo_2N) and studied the HER activity of Ru–Mo_2N (i.e., Ru_3–Mo_2N (100)) and Ru_3–Mo_2N (111) in both acidic and alkaline medium. From DFT calculations, they found that at the interfaces between the Ru_3 cluster and Mo_2N, charge redistribution takes place, which results in slight increases in the oxidation state of Ru. Additionally, the PDOS plot revealed a downshift of the Ru nanoclusters' d-band center, which decreases the binding strength of the reactive intermediates on the catalyst surface and is useful for tuning ΔG_H values. The ΔG_H values calculated on Ru_3–Mo_2N (111) was found to be −0.07 eV, which is much lowered compared to the ΔG_H values of −0.29 eV (on Ru_3 cluster), −0.3 eV (Ru_3–Mo_2N (100)), −0.52 eV (Mo_2N (100)), and −0.79 eV (Mo_2N (111)). Thus, the Ru_3–Mo_2N (111) crystal facet rendered the most catalytically active HER performance [27]. A pH universal catalyst, $RuRh_2$ bimetallene with rich structural defects, was designed by the Mu *et al.* group to study HER in both acidic and alkaline conditions. As we know, the thermodynamics of HER in an acidic medium is governed by ΔG_H values; in contrast, the dissociation of water in alkaline media is dependent on low activation energies (i.e., ΔG_B). The DFT studies on the $RuRh_2$ bimetallene system were conducted to explore ΔG_H and ΔG_B values. It was found that among the seven models (viz. Ru, Rh, Pt, $RuRh_2$/Ru sites, $RuRh_2$/Rh sites, $RuRh_2$/Ru sites with strain effect, and $RuRh_2$/Rh sites with strain effect) adopted, the optimal ΔG_H value was found for the $RuRh_2$ bimetallene/Ru system with Rh sites, which helped in facilitating the Volmer step on the surface of the catalyst. On the other hand, a lower ΔG_B

value of 0.33 eV was obtained on the $RuRh_2$ bimetallene/Rh site (with strain-induced effect) system compared to the $RuRh_2$/Ru (with strain-induced effect) sites (0.35 eV), $RuRh_2$/Rh sites (0.34 eV), Ru (0.63 eV), and Rh (0.64 eV) indicating that the dissociation of H_2O on the $RuRh_2$ surface is much simpler than on the Ru or Rh surface, which could significantly increase HER activity [28]. Liu and co-workers constructed Ni@Ni_2P–Ru catalysts for HER catalysis. Initially, they utilized DFT computations to anticipate the advantageous outcome of adding Ru into the Ni_2P system. They simulated systems/models viz. Ni_2P ternary system, the outer Ru-plane sites (Ni_2P–Ru-plane), Ru–Ni_2P interface edge sites (Ni_2P–Ru-edge), and the Ru-cluster sites (Ni_2P–Ru-cluster) for studying the thermodynamics of HER in detail on the catalyst surface. They found that the simulated Ni_2P–Ru-cluster shows energetically favorable H adsorption with a ΔG_H value of 0.01 eV compared to Ru (−0.21 eV), Ni_2P (−0.19 eV), Ni_2P–Ru-plane (−0.16) and Ni_2P–Ru-edge (−0.09 eV), which is nearly equal to the optimum ΔG_H value and thus results in enhanced HER performance [29]. Li *et al.* performed the orbital modulation on Ir (111) crystal facet to study the behavior of H_2 adsorption/desorption on the surface of the catalyst for achieving enhanced HER performance. A theoretical study suggests that an electronegative carbon/nitrogen (C/N) matrix can be used to modify Ir NPs, which will further boost the HER processes on the surficial Ir sites. The PDOS distribution of Ir and IrNC with H adsorbates on the surface reveals that hydrogen bonding is greater at the surficial Ir sites on IrNC. The free energy of H adsorption is found to be 0.25 eV at Ir sites and 0.04 eV for IrNC by maintaining the balance of the electronegative environment with C/N sites. This implies that hydrogen adsorption/desorption would favor the interaction energy between H and the IrNC surface more than that of Ir [30]. Luo *et al.* synthesized iridium nanorods (Ir–NR/C) by annealing Ir nanoparticles at 300°C, which acts as a bifunctional electrocatalyst [31]. In acidic HER catalysis (Figure 1.5a), according to DFT investigations, the IrO_X layer formed on Ir nanorods helped lower the ΔG_H value from 0.26 to 0.02 eV indicating that the layer's presence aided in the chemisorption of hydrogen ions in acidic HER. In an alkaline medium, the HER was theoretically calculated based on the following pathway: $H_2O \rightarrow H{-}OH \rightarrow H^* \rightarrow {}^*H{-}OH \rightarrow H_2$ (Figure 1.5b). The ΔG_B values for Ir–NR/C and Ir/C was calculated to be 0.49 and 0.91 eV, respectively. Thus, greater energy was needed to split the water molecules for active sites containing absorbed hydrogen ions. These results suggest that the Ir–NR/C electrocatalyst indicates a higher intrinsic HER activity than the uncalcined Ir/C electrocatalyst [31]. A nano dendritic structure of Ir–tungsten (IrW ND) alloy was synthesized by Lv *et al.* as an effective catalyst for a

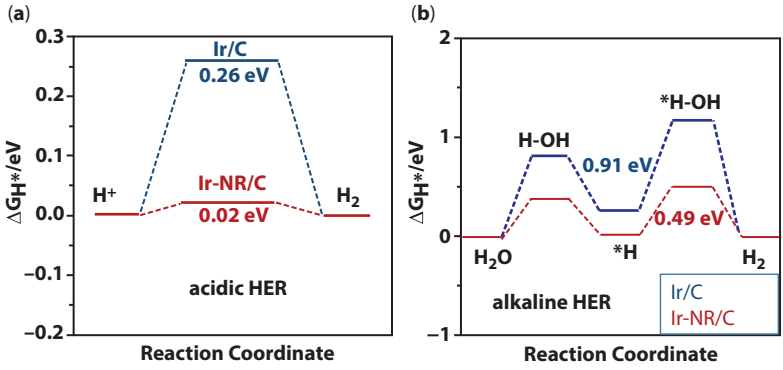

Figure 1.5 Computed free energy diagram of Ir/C and Ir–NR/C structures for HER in (a) acidic and (b) alkaline pH environment. *Reproduced with permission from Ref. [31]. Copyright (2020) Elsevier.*

pH-universal HER study [32]. Using first-principles calculations, he developed free energy diagrams to investigate the HER activity on IrW NDs. Both the binding energies of H (E_H) and OH (E_{OH}) adsorption on the catalyst surface were evaluated to get insights into the acidic and alkaline HER process. In acidic media, the most stable H adsorption was found on the top site of Ir for IrW NDs. The binding strength (E_H) for IrW NDs was found to be stronger than that for Ir but weaker than that for Pt indicating stronger adsorption of H on Ir active sites of IrW. In contrast, the E_{OH} value of IrW was calculated to be 0.61 eV, which is much lower than the E_{OH} values of Pt (0.88 eV) and Ir (1.13 eV). The increased affinity of the W active site for OH in an alkaline medium correlates with the lower barrier value of IrW. These characteristics allowed IrW to demonstrate superior HER activity in acidic and alkaline environments compared to Pt or Ir [32]. It has been reported that nitrogen-doped graphene sheets (Ir@N–G-750) coated with nanosized iridium nanoparticles exhibit strong HER activity in both acidic and alkaline environments. The first principle investigation of Wu *et al.* demonstrates how the pyridinic N synthesis might significantly lower the adhesion energy of carbon species doped with nitrogen [33]. The neighboring N atom's distance decreases and the Ir–N site begins to form as soon as the Ir cluster is introduced to the N–graphene system. The favorable active pyridinic N (−0.46 eV) adhered to the Ir surface modifies Gibbs free energy of hydrogen adsorption on Ir–N, in contrast to the pure Ir–graphene site (−2.72 eV) and the Ir–graphitic N (−0.77 eV). Consequently, N-doping helps to enhance the electrocatalytic performance of HER [33]. Mei *et al.* synthesized an efficient Ir-modified black phosphorous (BP)

electrocatalyst with favorable adsorption energies toward catalytic HER intermediates [34]. They found theoretically that the pristine BP and Ir catalyst exhibit hydrogen adsorption energies of 1.18 and −0.31 eV, respectively, which limits them to be an ideal HER catalyst. But when these two are coupled to form a BP/Ir heterostructure (IRBP), the ΔG_H value of IRBP significantly gets tuned to the −0.02 eV for acidic HER, which is very close to the ideal thermoneutral ΔG_H value of zero, and even remarkably outperforms the Pt (111) surface and individual Ir surface [34].

1.5.2 Oxygen Evolution Reaction (OER)

The oxygen evolution reaction (OER) process is the other half-cell reaction of the water splitting process. It involves a four-electron transfer reaction with sluggish electrode kinetics. This results in an undesirable free energy landscape of intermediates, such as *OH and *OOH, accounting for a significant loss in energy and efficiency. Therefore, it is of utmost importance to determine the rate-determining step (RDS) (which is the slowest step in the reaction mechanism that determines the overall rate of the reaction) as well as to decode which mechanism governs the catalytic process. These include the following reactions [35]:

$$2H_2O \leftrightarrow OH^* + H^+ + e^- + H_2O$$

$$OH^* + H^+ + e^- + H_2O \leftrightarrow O^* + 2H^+ + 2e^- + H_2O$$

$$O^* + 2H^+ + 2e^- + H_2O \leftrightarrow OOH^* + 3H^+ + 3e^-$$

$$OOH^* + 3H^+ + 3e^- \leftrightarrow O_2 + 4H^+ + 4e^-$$

The first term is related to the OER thermodynamic barrier, and the other term is related to the OER kinetics. Gibbs free energy change is a quantitative indicator that will provide the required energy and direction to produce a product from a group of reactants. Therefore, Gibbs free energy change for the four OER reactions is calculated as follows [35]:

$$\Delta G_1 = \Delta G_{HO^*} - \Delta G_{H2O} - eU - k_B T \ln (a_{H+}) + ZPE$$

$$\Delta G_2 = \Delta G_{O^*} - \Delta G_{HO^*} - eU - k_B T \ln (a_{H+}) + ZPE$$

$$\Delta G_3 = \Delta G_{HOO^*} - \Delta G_{O^*} - eU - k_B T \ln (a_{H+}) + ZPE$$